Numerical study of the dynamic properties of silica aerogels

Abdelali Rahmani[1], Philippe Jund[2], Claude Benoit[3, 4] and Rémi Jullien[2]

[1] Departement de Physique, Université Moulay Ismail, BP 4010 Meknès, Morocco
[2] Laboratoire de Science des Matériaux Vitreux, UMR 5587 CNRS, Université Montpellier II, Place Eugène Bataillon, 34095 Montpellier cedex 05, France
[3] Groupe de Dynamique des Phases Condensées, UMR 5581 CNRS, Université Montpellier II, Place Eugène Bataillon, 34095 Montpellier cedex 05, France

Abstract
We have developed a realistic model for silica aerogels based on a diffusion-limited cluster–cluster aggregation model in three dimensions with a primary particle represented by a sample of vitreous silica given by molecular dynamics simulations. Using the spectral moments method, with more than 30 000 computed moments, we calculated the densities of states and the dynamic structure factors of a simulated sample of silica aerogels of different macroscopic densities. We reproduce the vibration spectra experimentally obtained on basic silica, with a fracton region composed of two contributions associated with stretching and bond-bending modes respectively. The spectral dimensions describing these contributions are close to the measured values. The analysis of our numerical results in the light of the scaling argument is reported.

1. Introduction

Silica aerogels are quite appreciated in a number of high technology areas. The need to obtain a better understanding of these systems has led to several experimental (Courtens *et al* 1987, 1988, Reichenauer *et al* 1989, Vacher *et al* 1990, Anglaret *et al* 1994, Courtens and Vacher 1997), theoretical (Alexander and Orbach 1982, Alexander 1989 and Alexander *et al* 1993) and numerical (Hasmy *et al* 1993, 1994, Nakayama *et al* 1994, Rahmani *et al* 1994, 1995, 1996, 1998, Stoll *et al* 1992, Viliani *et al* 1995) studies. These studies have revealed the structural and dynamic properties of these systems.

In the last decade, fractals have attracted considerable interest because of their potential for describing a wide range of non-regular structures. Dynamic scaling has been applied to the dynamics of fractal structures. To describe the vibrational density of states (DOS) $g(\omega)$ of

[4] Corresponding author.

these systems, Alexander and Orbach (1982) introduced the spectral dimension $\tilde{d}$ for fracton modes:

$$g(\omega) \propto \omega^{\tilde{d}-1}. \tag{1}$$

To obtain further information on the dynamics of fractal structures, Alexander *et al* (1993) studied the dynamic structure factor $S(q, \omega)$ of these systems without any specific structure model in the case of scalar elasticity. Based on the single length scale postulate (SLSP), they showed that $S(q, \omega)$ should have the following scaling form:

$$S(q, \omega) = q^y H(q\lambda(\omega)) \tag{2}$$

where the single length $\lambda(\omega)$ scale follows the dispersion relation

$$\lambda(\omega) \propto \omega^{-\tilde{d}/D}. \tag{3}$$

H is a scaling function and D is the fractal dimension of the system. In homogeneous systems, $\tilde{d}$ and D correspond to the Euclidean dimension d.

In order to test the validity of these dynamic scaling arguments, we have previously published results concerning different simulated structures (Rahmani *et al* 1995, 1996; see also Stoll *et al* 1992). There was excellent agreement with theory.

Different experimental studies suggested that silica aerogels are excellent systems for investigating fractal vibrations. Combining neutron, Raman and Brillouin spectroscopies, Vacher *et al* (1990) identified a succession of regimes in the vibrational spectra of silica aerogels. Besides the phonon–fracton ($\omega_c/2\pi \approx 1$ GHz) and fracton–particle ($\omega_c/2\pi \approx 250$–$600$ GHz) mode crossovers, they find an additional crossover ($\omega_c/2\pi \approx 10$ GHz) that suggests two distinct elastic regimes in the fracton range. Based on the work of Feng (1985), the authors supposed that when $\omega_e < \omega < \omega_a$, the fracton properties of the system are governed by bond-stretching motion, which scales the same way as the scalar model with $\tilde{d}_s = 1.9$–2.2, whereas, when $\omega_c < \omega < \omega_e$, bond-bending motions are dominant with an effective spectral dimension $\tilde{d}_b = 0.9$–1.3. Phonons and particle modes are given for $\omega < \omega_c$ and $\omega > \omega_a$ respectively.

Using small-angle neutron scattering (SANS), Vacher *et al* (1990) showed that porous silica aerogels are made up of a disordered array of connected fractal clusters resulting from primary-particle aggregation. These systems reveal a fractal structure for a wide range of densities with fractal dimension $D = 1.8$–2.4. The primary-particle structure is similar to vitreous silica (v-SiO$_2$). Basic and neutral aerogels can be distinguished according to the pH of the aqueous hydrolysis solution. Basic aerogels are made of larger-sized (≈ 20 Å), but strongly polydispersed, primary particles. SANS and simulations (Anglaret *et al* 1994, Hasmy *et al* 1994, Rahmani *et al* 1996) of base-catalysed aerogels show that excellent fits of the scattering intensity are obtained with the diffusion-limited cluster–cluster aggregation (DLCA) structure fractal model (Botet *et al* 1983, Jullien and Botet 1987, Hasmy *et al* 1993, 1994). The fractal dimension of the DLCA built in three dimensions is $D = 1.8$.

In a previous work (Rahmani *et al* 1994), we developed a model for silica aerogels based on infinite percolating clusters, with a homogeneous particle represented by a small sample of v-SiO$_2$ given by molecular dynamics simulation (MD). Based on the Born–Mayer–Higgins potential (Garofalini 1982, Feuston and Garofalini 1988), our models, where we supposed that each site of the percolating cluster was occupied by a sample of v-SiO$_2$, showed that it is difficult to clearly reproduce contributions of the DOS of silica aerogels. The use of the percolation structure model is inadequate for silica aerogel structure. The analysis of vibrational spectra in terms of spectral dimensions involves building a model based on another structure such as DCLA for basic aerogels.

A primary goal of this work was to reproduce the measured DOS and inelastic scattering intensity obtained in small-angle neutron scattering (SANS), from a realistic fractal model for

silica aerogels. To do this, it is not only necessary to work on a very large system able to generate fractons of up to 1 GHz, but we must also have an efficiency computational code to treat these systems. Note that this explored frequency region ($\approx$1 GHz) corresponds to $3/10^5$ of the maximal frequency $\omega_{max} \approx 35\,000$ GHz of the spectrum.

To calculate the total DOS and dynamic structure factor, we used the spectral moments method (Benoit *et al* 1992), which is a powerful tool for determining the linear response (infrared, Raman and inelastic neutron scattering) of harmonic systems. When applied to the calculation of total DOS for very large systems, the method presents some difficulties at very low frequencies. Indeed, as shown in Benoit *et al* (1992), a sharp truncation of the fraction (200 moments) causes the appearance of sharp lines in the calculated spectrum. However, the calculations show that a greater number of moments are required to obtain the best results. Thanks to the hierarchical parallel computation technique and the size of supercomputers, we can actually calculate more than 30 000 moments for very large systems (more than 10^6 degrees of freedom) during a real time of less than 24 h on an IBM SP2 computer.

In this paper, we present a model of silica aerogels based on a DLCA structure model in three dimensions with a primary particle represented by a sample of v-SiO$_2$ given by molecular dynamics simulations (Jund and Jullien 1999, Jund *et al* 2000). We report results of the densities of states and dynamic structure factors performed for samples of different macroscopic density. In the light of the scaling argument, we deduced values for the required scaling exponents. Comparisons with results obtained for silica aerogels are reported.

In section 2, we describe our physical model for silica aerogels. The used structure and interaction potential are presented. In section 3, we present the results of our calculations of DOS and the inelastic neutron scattering intensity of our systems. We also briefly review scaling arguments concerning the dynamic structure factor. Finally, in section 4, we discuss our numerical results in the light of scaling arguments and experimental results obtained for silica aerogels.

2. Physical model

2.1. Structure

In order to take into account the fractal nature of the structure of silica aerogels, we suppose in our model that the networks of our systems are represented by a three-dimensional (3D) DLCA lattice model. As showed by simulation (Hasmy *et al* 1994, Rahmani *et al* 1996), this model is adequate to reproduce properties of basic silica aerogels. To generate a 3D DLCA aggregate, initially, we randomly dispose n identical primary particles on sites of a cubic lattice, within a cubic box of edge length l. For a sufficiently high particle concentration ($c = n/l^3$), one can obtain a gelling network at the end of the aggregation process. The final configuration consists of a disordered array of interconnected fractal aggregates. It has been shown (Hasmy *et al* 1994) that the mean size ξ of aggregates decreases as the concentration c increases according to

$$\xi \propto c^{-1/(3-D)} \tag{4}$$

where the fractal dimension D of 3D DLCA is close to 1.8.

To complete our structural model and according to silica aerogel experiments, we considered that the primary particle of the 3D DLCA aggregate is represented by a sample of v-SiO$_2$ obtained by MD simulation at 300 K (Jund and Jullien 1999). In this work, our primary particle is a 648-atom (216 silicons and 432 oxygens) system with a box length of 20.5 Å. Using MD simulation with a pair potential given by equation (5), one can reproduce a

similar structure to that determined from x-ray diffraction and neutron scattering experiments for v-SiO$_2$. The O–Si–O angle distribution is found to peak sharply around the tetrahedral angle, while the Si–O–Si angles are broadly distributed between $115°$ and $180°$, with a mean of $150°$ in agreement with the experimental predictions. The radial distribution function and structure factor $S(q)$ were also found to be in accord with the diffraction and scattering results (Jund *et al* 2000).

2.2. Potential

The potential used in this study is given by the Beest–Kramer–Santen (BKS) equation (Van Beest *et al* 1990), which was used in the MD simulation to understand the microscopic structure and dynamics of v-SiO$_2$. One of the advantages of the BKS pair potential is that it is easy to implement in simulations due to its simple analytical form. The interaction between atoms i and j is given by

$$V_{ij}(r_{ij}) = q_i q_j / r_{ij} + A_{ij} \exp(-B_{ij} r_{ij}) - C_{ij}/r_{ij}^6 \tag{5}$$

with r_{ij} representing the distance between atoms i and j, q_i the electronic charge of atom i and A_{ij}, B_{ij} and C_{ij} fixed as follows: $A_{SiO} = 18\,003.7572$ eV and $A_{OO} = 1388.773$ eV; $B_{SiO} = 4.873\,18$ Å^{-1} and $B_{OO} = 2.76$ Å^{-1}; $C_{SiO} = 133.5381$ eV Å^6 and $C_{OO} = 175.0$ eV Å^6. This potential consists of a Coulomb term and a covalent (short-range) contribution. The condition of charge neutrality fixes q_{Si} ($q_{Si} = +2.4e$) and q_O ($q_O = -1.2e$). Only two different short-range interactions are allowed: Si–O to describe the silica bond and the O–O non-bonded interaction, which modifies the Coulomb repulsion and ensures the tetrahedral arrangement of oxygen atoms around the silicon atom. The nearest-neighbour cut-off for all interactions is equal to 7 Å.

So, if $u_\alpha(l, i)$ denotes the displacement of atom i of particle l in the α direction, the set of equations of motion for atom i is given by

$$m_i \ddot{u}_\alpha(l, i) = -\sum_{m,\beta,j} \Phi_{\alpha\beta}(l, m, i, j) u_\beta(m, j) \qquad (\alpha = 1, 2 \text{ and } 3) \tag{6}$$

with

$$\Phi_{\alpha\beta}(l, l, i, i) = -\sum_{m,j}' \Phi_{\alpha\beta}(l, m, i, j)$$

where $\Phi_{\alpha\beta}(l, m, i, j)$ are the force constants between atoms i (particle l) and j (particle m) given by

$$\Phi_{\alpha\beta}(l, m, i, j) = \left[\frac{r_\alpha r_\beta}{r^2} \left(\frac{1}{r} \frac{\partial V_{il,jm}}{\partial r} - \frac{\partial^2 V_{il,jm}}{\partial r^2} \right) - \delta_{\alpha\beta} \frac{1}{r} \frac{\partial V_{il,jm}}{\partial r} \right]_{r=|r_i(l)-r_j(m)|}. \tag{7}$$

m_i and $r_i(l)$ are respectively the mass and the equilibrium position of the ith atom in the lth particle.

In this work, we present results obtained for three samples of different concentrations $c = 0.04, 0.06$ and 0.08 constructed via the 3D DLCA model on cubic lattice of edge size $l = 30$. These concentrations correspond to the aerogel density according to the formula

$$\rho = c\rho_0 \tag{8}$$

where $\rho_0 = 2.2$ g cm^{-3} is the density of vitreous silica. Hence, our three simulating samples, denoted A, B and C, have densities $\rho = 0.088$ g cm^{-3}, $\rho = 0.132$ g cm^{-3} and $\rho = 0.176$ g cm^{-3} respectively. The box edge size of these systems is $L = 615$ Å. We also performed calculations on a cubic lattice, with periodic conditions, of side $l = 5$ ($L = 102.5$ Å) for concentration $c = 1$ ($\rho_0 = 2.2$ g cm^{-3}), denoted D.

3. Numerical results

Using the spectral moments method, we developed calculations of DOS $g(\omega)$ and the dynamic structure factor $S(q, \omega)$ for the three samples A, B and C of our model for silica aerogels. The computed DOS of the system D is reported.

In table 1, we present the dimensions X, Y and Z, the macroscopic densities ρ and the order N (degrees of freedom) of the dynamic matrix **D** of our aggregates. We have also given the memory occupation and the real CPU time necessary to compute one coefficient set (a_n, b_n) of the continued fraction for each system. Our parallel codes run on nine nodes of 256 Mb each. We note very good stability in calculation of the coefficients (a_n, b_n).

Table 1. Characteristics of simulated samples: X, Y and Z designate dimensions of the aggregates, ρ is the macroscopic density, N is the size of **D** for the four samples A, B, C and D; CPU is the real time necessary to compute one moment; memory is the memory storage required for each system using the spectral moments method by node.

Sample	l	X (Å)	Y (Å)	Z (Å)	CPU (s)	Memory (Mb/node)	N	ρ (g cm^{-3})
A					14	70	2.0995×10^6	0.088
B	30	615	615	615	21	110	3.1473×10^6	0.132
C					28	150	4.1990×10^6	0.176
D	5	102.5	102.5	102.5	9	10	0.2430×10^6	2.200

In the following, we only present our numerical results for DOS and the dynamic structure factor of our systems. The discussion and comparisons of these results with other works will is presented in the next section.

3.1. Density of states

In figure 1, we have plotted the results of the calculated density of states $g(\omega)$ versus the frequency $\omega/2\pi$ for the isolated homogeneous particle (648 atoms) considering the cases in which we exclude or not the periodic conditions (P.C.) in the dynamic matrix calculations. As shown, the spectrum of DOS without P.C. presents (qualitatively) the same behaviours as the spectrum obtained with P.C., which is in agreement with other simulation results and experimental data of vitreous silica (Guillot and Guissani 1997, Jund and Jullien 1999). It is clearly not possible to impose periodic boundary conditions on each particle in a fractal lattice and atoms at the surface are certainly not all in stable position. However, computations with an isolated particle highlighted very few imaginary frequencies (one or two out of about 2000). Furthermore, in fractal lattices, every particle is in contact with one to six other surrounding particles and thus surface atoms are often in stable positions. Note especially that we specifically study very large extended modes.

In figure 2, we have plotted DOS $g(\omega)$ against $\omega/2\pi$, on a decimal log–log scale, for the four systems A, B, C and D defined in table 1. We have also reported (from Vacher *et al* 1990) the DOS of a neutral aerogel (N) with density $\rho = 0.210$ g cm^{-3} in the inset. The same behaviour is noted between the computed DOS and measured vibrational spectra of silica aerogels. Thus, we observe that in the high frequency region $\omega > \omega_a$, the four computed curves show a common region which clearly represents the particle modes. This value for $\omega_a/2\pi \approx 400$ Ghz is in agreement with experimental results concerning silica aerogels with mean particle radius $R \approx 10$ Å. For $\omega < \omega_a$, the D system (vitreous silica) spectrum presents a Debye law according to properties of homogeneous systems, whereas in
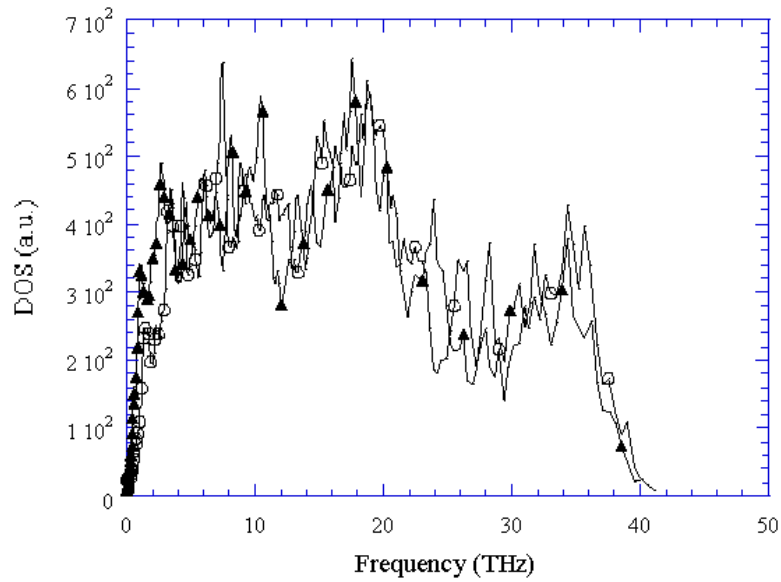
Figure 1. DOS $g(\omega)$ versus $\omega/2\pi$ for the 648-atom isolated homogeneous particle: —⊖—, with P.C.; —▲—, without P.C.
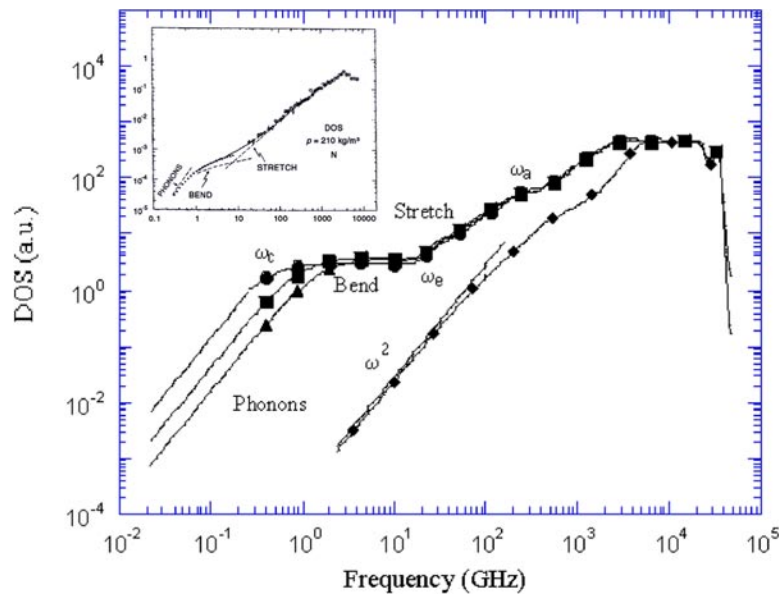

Figure 2. DOS $g(\omega)$ versus $\omega/2\pi$, on a log–log scale for the three samples denoted A, B, C and D, of densities $\rho = 0.088, 0.132, 0.176$ and 2.2 g cm^{-3}. Inset: vibrational spectrum for a neutral (N) silica aerogel ($\rho = 0.21$ g cm^{-3}) as described in Vacher *et al* (1990). —●—, A; —■—, B; —▲—, C; —◆—, D.

the intermediate frequency region two contributions are observed with a supplement crossover frequency $\omega_e/2\pi \approx 15$ GHz. For $\omega > \omega_e$, our systems A, B and C present an effective linear regime, which can be described by the power law $g(\omega) \propto \omega^{1.04\pm0.03}$. For $\omega_c < \omega < \omega_e$, the
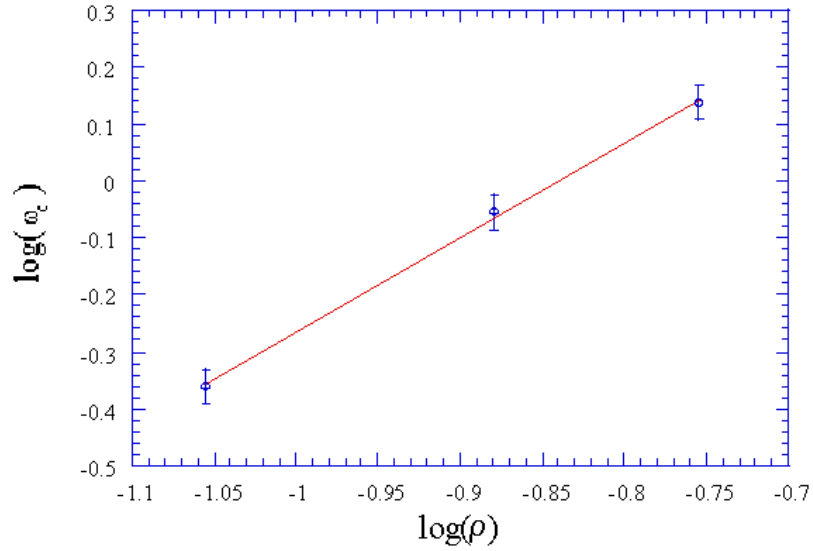
Figure 3. The crossover frequency ω_c versus the macroscopic density ρ on a log–log scale.

spectra present an effective linear regime following the scale form $g(\omega) \propto \omega^{0.06\pm0.03}$. As the macroscopic density ρ increases, we observe an increase in the crossover frequency ω_c. A Debye law in the very low frequency region $\omega < \omega_c$ can be expected. We note that for the weakly dense system ($\rho = 0.088$ g cm^{-3}), the crossover frequency ω_c is in the 1 GHz range, as in experimental conditions.

In figure 3, we have represented the function $\log(\omega_c)$ versus $\log(\rho)$. One can deduce that the frequency crossover ω_c follows the power law

$$\omega_c \approx \rho^{1.66\pm0.03}. \tag{9}$$

ω_c are given by the intersection of straight lines of the bending regime and the expected Debye law.

As argued in Feng (1985), DOS $g(\omega)$ is Debye-like for $\omega < \omega_c$ and complies with the power law

$$g(\omega) = [C_s]^{-3}\omega^2 \tag{10}$$

where C_s is the Debye averaged sound velocity.

In figure 4, we have represented the function $\log(C_s)$ versus $\log(\rho)$. This result reproduces the experimental data concerning the increase in sound velocity with increasing ρ. Supposing that the sound velocity is $C_s \approx 4000$ m s^{-1} in vitreous silica then for the weakly dense system $C_s \approx 255$ m s^{-1}. We observe the following power law:

$$C_s \approx \rho^{0.86\pm0.03}. \tag{11}$$

Qualitatively, this behaviour is consistent with results obtained for basic silica aerogels (Anglaret *et al* 1995).

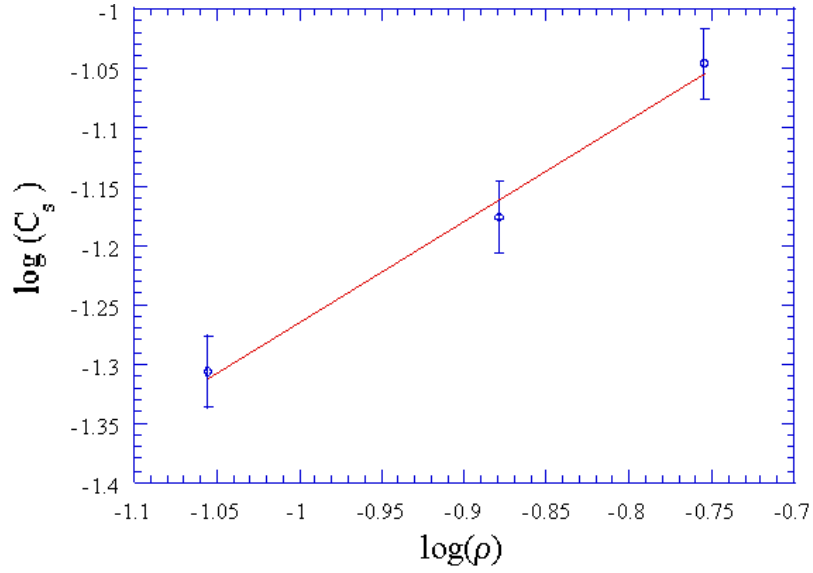**Figure 4.** The sound velocity C_s versus the macroscopic density ρ on a log–log scale.

3.2. Dynamic structure factor

3.2.1. Scaling arguments. The inelastic cross-section is directly related to the displacement–displacement correlation function $I(q, \omega)$, given by

$$I(\vec{q}, \omega) = (n(\omega) + 1) \sum_j |a_j(\vec{q})|^2 \frac{(\delta(\omega - \omega_j) - \delta(\omega + \omega_j))}{2\omega_j}$$

$$\approx \frac{kT}{\omega^2} \sum_j |a_j(\vec{q})|^2 \delta(\omega - \omega_j) \tag{12}$$

for $\omega > 0$, with $(n(\omega) + 1) \approx kT/\omega$ and

$$a_j(\vec{q}) = \sum_{n\alpha} \frac{b_n}{\sqrt{m_n}} q_\alpha \langle \alpha n \mid j \rangle \exp(\mathrm{i}\vec{q}\vec{r}_n) \tag{13}$$

where $\vec{r}_n$, m_n and b_n are, respectively, the equilibrium position, the mass and scattering length ($b_O = 5.8$ and $b_{Si} = 4.14$) of the nth atom, ω_j and $\langle \alpha n \mid j \rangle$ are the frequency and the (αn) components of the eigenvector $|j\rangle$ of the jth mode, $\alpha = x, y, z$ are the Cartesian indices, kT is the thermal energy and q_α is the component α of $\vec{q}$.

The dynamic structure factor $S(q, \omega)$ is defined by

$$S(q, \omega) = \sum_j |a_j(\vec{q})|^2 \delta(\omega - \omega_j). \tag{14}$$

As proposed by Alexander *et al* (1993), assuming that the SLSP is valid, in the case of scalar elasticity, the dynamic structure factor $S(q, \omega)$ has the universal scaling form (2) and complies with the asymptotic behaviour in the $q\lambda \ll 1$ limit,

$$S(q, \omega) \propto q^\gamma \omega^{-\alpha} \tag{15}$$

where $\gamma = 4$ and $\alpha = 1 - (2\sigma - 4)\tilde{d}/D$, σ being a scaling index describing modulation of the density in the embedding space by the vibration. In the $q\lambda \gg 1$ limit, $S(q, \omega)$ involves two contributions:

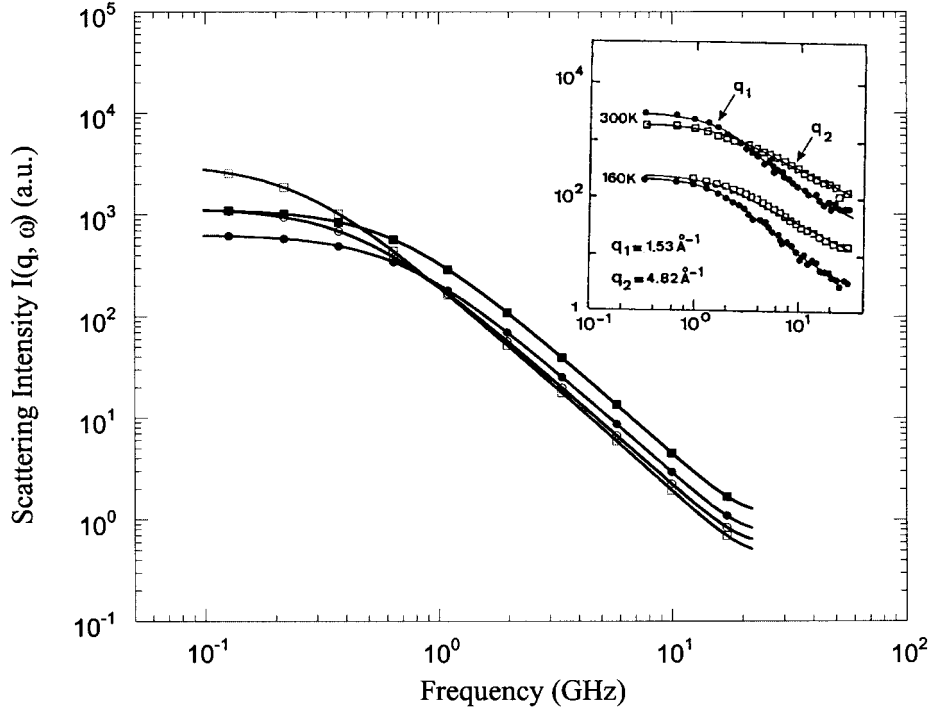$$S(q, \omega) = S_1(q, \omega) + S_2(q, \omega) \tag{16}$$

Figure 5. The scattering intensity $I(q, \omega)$ versus the frequency $\omega/2\pi$ on a log–log scale for four values of the wave-vector q (Å^{-1}) for the A sample: —⊖— 1 = 0.1168, —⊟— q = 0.4672, —●— q = 0.584, —■— q = 1.1168. Inset: inelastic neutron scattering spectra for two (T = 160 K and T = 300 K) basic (B) silica aerogels (ρ = 0.095 g cm^{-3}) as described in Vacher *et al* (1990).

where the functions $S_1(q, \omega)$ and $S_2(q, \omega)$ obey the power laws

$$S_1(q, \omega) \propto q^{\delta_1} \omega^{\beta_1} \qquad \text{with } \beta_1 = \tilde{d} - 1 \text{ and } \delta_1 = 2\sigma - D \qquad (17a)$$

and

$$S_2(q, \omega) \propto q^{\delta_2} \omega^{\beta_2} \qquad \text{with } \beta_2 = 2\sigma\tilde{d}/D + \tilde{d} - 1 \text{ and } \delta_2 = -D. \qquad (17b)$$

3.2.2. Results. In figure 5, we report, on a log–log scale, the frequency dependence of intensity $I(q, \omega)$ for our sample A of density $\rho = 0.088$ g cm^{-3} for four typical curves corresponding to values of the wave-vector modulus q: $q = 0.1168, 0.4672, 0.584$ and 1.1168 Å^{-1}. The abscissa indicates the frequency $\omega/2\pi$. In order to compare the calculated and experimental data, we present in the inset (from Vacher *et al* 1990) the inelastic neutron scattering measured data for basic silica aerogel (B) density $\rho = 0.095$ g cm^{-3} at two values of q (1.53 Å^{-1}, 4.82 Å^{-1}) and two temperatures ($T = 160$ K and $T = 300$ K).

In figure 6, we have plotted, for several q-values ($q = 0.0097, 0.0292, 0.1168, 0.292, 1.168$ and 2.92 Å^{-1}), the reduced dynamic structure factor $\bar{S}(q, \omega) = S(q, \omega)/q^2$ versus frequency, on log–log scale, for sample A. In the low frequency region ($\omega/2\pi < 50$ GHz), for each q-value, all curves exhibit the same form, similar to DOS behaviour. In the intermediate frequency region ($\omega_e < \omega < \omega_a$), we observe that as soon as q increases, a regime with a positive slope appears in the low-frequency region to the detriment of the decreasing high-frequency regime. Two regions can thus be distinguished in stretching regime fracton modes.
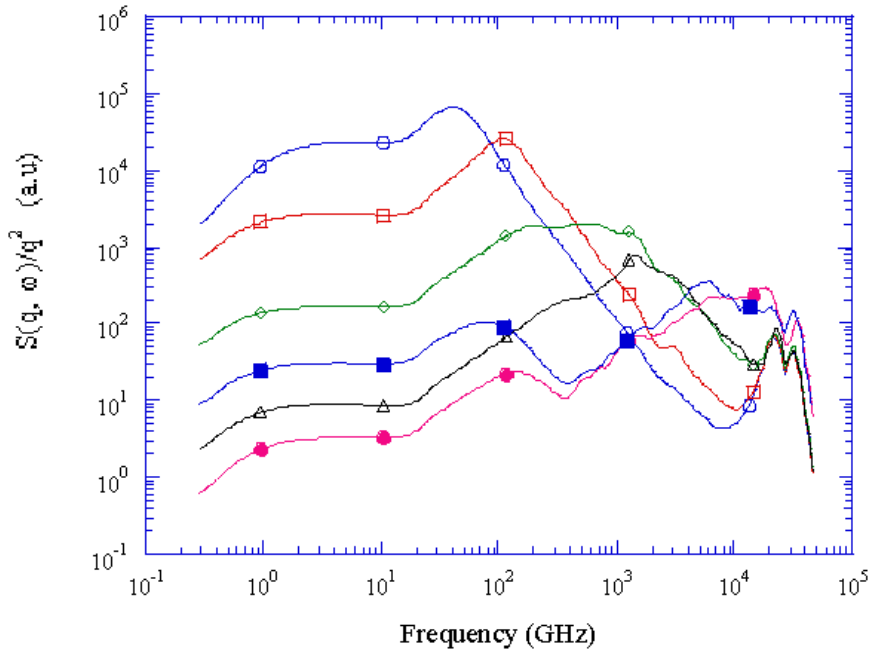
Figure 6. The reduced dynamic structure factor $\bar{S}(q, \omega) = S(q, \omega)/q^2$ versus $\omega/2\pi$, on a log–log scale, for sample A of density $\rho = 0.088$ g cm^{-3} for six values of the wave-vector modulus q (Å^{-1}): –⊖–, 0.0097; –⊟–, 0.0292; –◇–, 0.1168; –△–, 0.2920; –●–, 1.1168; –■–, 2.920.

If ω_0 denotes the frequency at which $S(q, \omega)$ has a maximum value for each fixed wave-vector q, as $q\lambda(\omega_0) = 1$, the case where $\omega \gg \omega_0$ ($\omega \ll \omega_0$) corresponds to the $q\lambda \ll 1$ ($q\lambda \gg 1$) limit. In this region, we note that at low q-values, the dynamic structure factor is mostly dominated by a decreasing linear regime ($\omega \gg \omega_0$), whereas at larger q, the linear increasing regime is dominant ($\omega \ll \omega_0$). The frequency dependence of the global dynamic structure factor $\bar{S}(\omega) = \sum_q \bar{S}(q, \omega)$ given by averaging several q-values, can be expressed as

$$\bar{S}(\omega) \propto \omega^{-2.05\pm0.05} \qquad \text{for } q\lambda \ll 1 \tag{18a}$$

and

$$\bar{S}(\omega) \propto \omega^{0.97\pm0.05} \qquad \text{for } q\lambda \gg 1. \tag{18b}$$

Let us consider the wave-vector dependence of $S(q, \omega)$. In order to compare our numerical results to the experimental dynamic structure factor for silica aerogels, we have reported in figure 7 the variation in $S(q, \omega)$ versus q for the A sample for five fixed frequencies $\omega/2\pi$: 12.7, 20.8, 34.0, 55.5 and 90.7 GHz. In the inset, we have reported (from Reichenauer *et al* 1989), the experimental and theoretical (full line) dynamic structure factors for different frequencies for a basic aerogel of density $\rho = 0.250$ g cm^{-3}.

For the analysis of our spectra in terms of scaling arguments (Alexander *et al* 1993), in figure 8 we have plotted, on a log–log scale, $\bar{S}(q, \omega)$ versus q for the A sample for some frequency values: 20.8, 34, 90.7, 242.1, 395.6, 646.4, 1056.2 and 1725.8 GHz. We observe that as soon as ω increases a regime with a positive slope appears in the low q-value region to the detriment of the decreasing high q-value regime.

In order to check the q-index scaling of $S(q, \omega)$, we determined, for each frequency ω, the wave-vector modulus q_0 for which $\bar{S}(q, \omega)$ has the maximum value. $\bar{S}(q, \omega)$ values
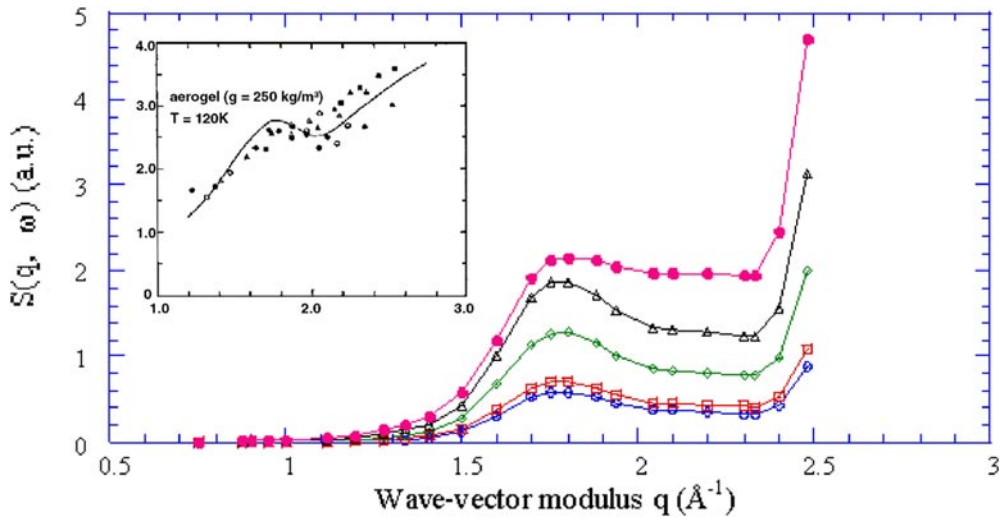
Figure 7. The reduced dynamic structure factor $S(q, \omega)$ versus q, for sample A of density $\rho = 0.088$ g cm^{-3} for five values of the frequency $\omega/2\pi$: $-\ominus-$, 12.7 GHz; $-\boxdot-$, 20.8 GHz; $-\diamondsuit-$, 34.0 GHz; $-\triangle-$, 55.5 GHz; $-\bullet-$, 90.7 GHz. Inset: the dynamic structure factors $S(q, \omega)$ for basic silica aerogels ($\rho = 0.25$ g cm^{-3}) as described in Reichenauer *et al* (1989).
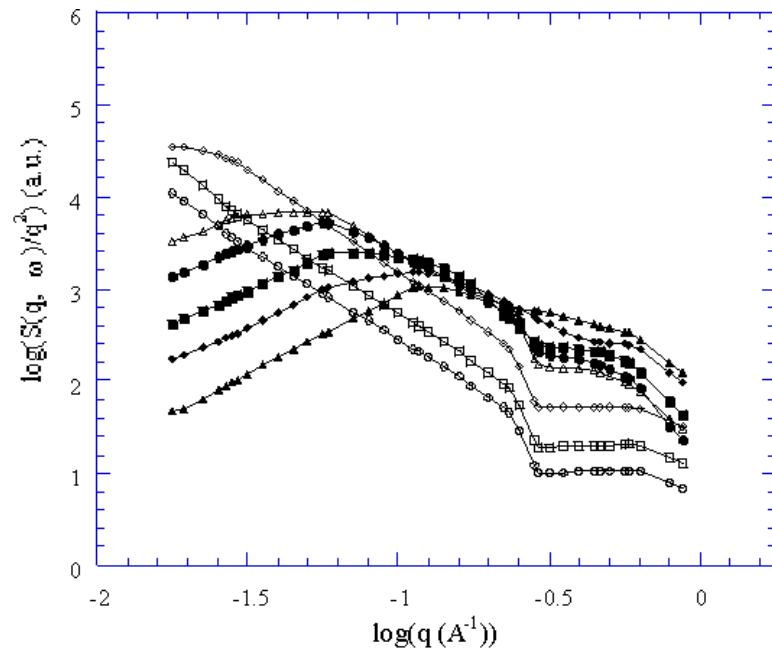

Figure 8. The reduced dynamic structure factor $S(q, \omega)/q^2$ versus q, on a log–log scale, for sample A of density $\rho = 0.088$ g cm^{-3} for eight values of the frequency $\omega/2\pi$: $-\ominus-$, 20.778 GHz; $-\boxdot-$, 33.953 GHz; $-\diamondsuit-$, 90.658 GHz; $-\triangle-$, 242.07 GHz; $-\bullet-$, 395.55 GHz; $-\blacksquare-$, 646.35 GHz; $-\blacklozenge-$, 1056.2 GHz; $-\blacktriangle-$, 1725.8 GHz.

are then rescaled by $\bar{S}(q_0, \omega)$ and averaged over ω to give the function $\bar{S}(q) = S(q)/q^2 = \frac{1}{n} \sum_{\omega=1}^{n} (\bar{S}(q, \omega)/\bar{S}(q_0, \omega))$ (Rahmani *et al* 1996). The results demonstrate that the wave vector
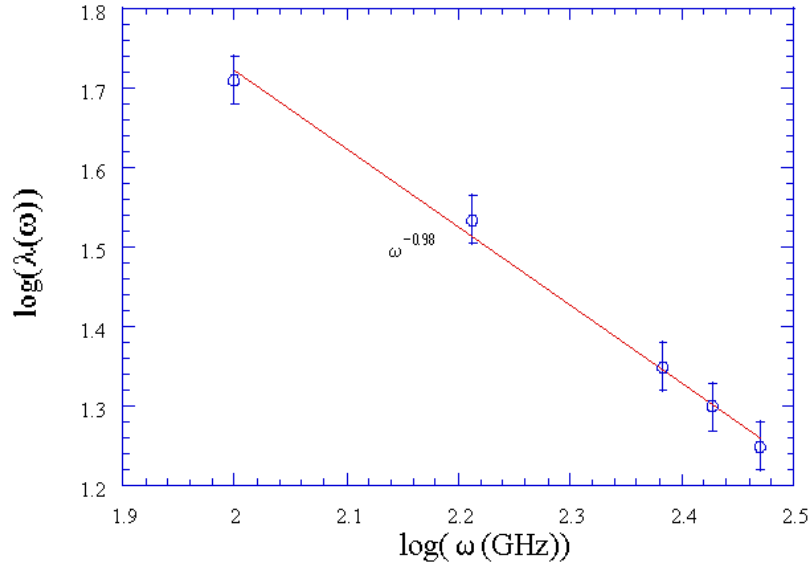
Figure 9. The values of wavelength $\lambda(\omega) \propto 1/q_0$ plotted as a function of frequency $\omega/2\pi$, on a log–log scale, for the sample of density $\rho = 0.088$ g cm^{-3}.

dependence complies with the power law

$$\bar{S}(q) \propto q^{1.7 \pm 0.1} \qquad \text{for } q \text{ below } q_0 \tag{19a}$$

and

$$\bar{S}(q) \propto q^{-2.1 \pm 0.1} \qquad \text{for } q \text{ above } q_0. \tag{19b}$$

Finally, in figure 9, we have plotted, on log–log scale, the length scale $\lambda \propto 1/q_0$ versus the frequency ω for the A sample. As indicated by the full line, we observe that the scaling length complies with the power law:

$$\lambda(\omega) \propto \omega^{-0.98 \pm 0.03} \tag{20}$$

4. Discussion and conclusion

In this paper, we have studied the dynamic properties of a realistic model for silica aerogels. This model is based on a lattice cubic DLCA fractal structure in three dimensions where the primary particle is represented by a vitreous silica sample of 648 atoms, confined in a box, given by molecular dynamics simulation. The studied samples can be compared to experimental samples of studied silica aerogels (size greater than 600 Å and densities from $\rho = 0.088$ g cm^{-3} to $\rho = 0.176$ g cm^{-3}). Using the spectral moments method and its parallel code form, we have calculated the densities of states and dynamic structure factors of our systems with accuracy up to 1 GHz.

The analysis of our numerical results of DOS in the light of a scaling theory proposed by Alexander and Orbach (1982) and Feng (1985), shows that the vibrational spectra of our system presents two different contributions in frequency regions delimited by crossovers ω_c and ω_a. In the frequency region $\omega_e < \omega < \omega_a$, the spectra present a linear fracton regime governed by an effective spectral dimension $\tilde{d}_s = 2.04 \pm 0.03$ usually associated with stretching modes. For $\omega_c < \omega < \omega_e$, the spectra present a fracton regime, usually associated with bond-bending

motions, with a spectral dimension $\tilde{d}_b = 1.06 \pm 0.03$. The calculated spectral dimension values for our models are close to measured values for basic silica aerogels ($\tilde{d}_s \approx 1.9$ and $\tilde{d}_b \approx 1.0$: Vacher *et al* 1990), for which the mean particle radius was ~10 Å. The phonon–fracton crossover ω_c is around 1 GHz, in agreement with Brillouin's experiments. We also note close agreement between the computed value of the fracton–particle mode crossover $\omega_a/2\pi \approx 400$ GHz and the measured values. The experimental value $\omega_e/2\pi \approx 10$ GHz is close to the computed one $\omega_e/2\pi \approx 15$ GHz.

To test the accuracy of our calculation with scaling arguments, we now consider the scaling laws (9) and (11). Combining the relations (3) and (4), one can deduce the scaling law (Courtens and Vacher 1997)

$$\omega_c \propto \rho^{D/\tilde{d}_b(3-D)}. \tag{21}$$

With the bond-bending spectral dimension value $\tilde{d}_b = 1.06 \pm 0.03$ deduced from the scaling behaviour of the DOS, from power law (9) one can find that $D = 1.91 \pm 0.05$.

On the other hand, the sound velocity obeys the scaling law (Courtens and Vacher 1997),

$$C_s \propto \rho^{\tilde{d}_b - D/\tilde{d}_b(D-3)}. \tag{22}$$

From the power law (11), we find that the fractal dimension $D = 1.98 \pm 0.05$, with the same value $\tilde{d}_b = 1.06 \pm 0.03$, is close to the value deduced from equation (21).

The average value of $D = 1.95 \pm 0.05$ closely agrees with the fractal dimension of DLCA in three dimensions. We note also that this obtained fractal dimension for our model is near the fractal dimension value of some basic silica aerogels.

From Anglaret *et al* (1995), the sound velocity in silica aerogels varies with an exponent ranging from 0.43 to 1.41. The computed value 0.86 (equation (11)) for our model is consistent with these values.

The comparison of our result for the dynamic structure factor with the experimental measurement of Reichenauer *et al* (1989) shows a qualitative similarity (figure 7). In addition, good agreement is also obtained for scattering intensity as indicated in figure 8 compared to experimental spectra of silica aerogels (Vacher *et al* 1990).

To discuss our results on the dynamic structure factor in the light of the scaling theory of Alexander *et al* (1993), we observe in figure 8 that the bond-bending mode region is similar for all curves for fixed wave-vector q ($q > 0.0087$ Å^{-1}) and similar to the DOS spectra, whereas in the stretching fracton mode region the dynamic structure factor complies with a power law $S(q, \omega) \propto q^\gamma \omega^{-\alpha}$ with $\gamma = 3.7 \pm 0.1$ and $\alpha = 2.10 \pm 0.05$ in the $q\lambda \ll 1$ limit. In the $q\lambda \gg 1$ limit, we have the scaling form $S(q, \omega) \propto q^\delta \omega^\beta$ with $\delta = -0.10 \pm 0.10$ and $\beta = 0.97 \pm 0.05$. The γ-value is close to 4 as expected in equation (15) and identical to the value obtained for 3D DLCA in the case of scalar elasticity (Rahmani *et al* 1996). We can also note that the α-value (≈ 2.3) obtained for these systems is close to the value of our realistic model in this region of frequencies, which could actually be associated with the stretching modes. This also confirms the validity of the scaling law proposed by Alexander *et al* (1993) in the $q\lambda \ll 1$ limit. In the $q\lambda \gg 1$ limit, the δ-value (0.21) and β-value (0.4) for 3D DLCA with scalar model are substantially different from the values of our model. This difference could be associated with the tensorial nature of interactions induced by the used potential.

To test the coherence of our computed indices in stretching regime modes from scaling laws (20) and (3) and using the average fractal dimension $D = 1.95 \pm 0.05$, we deduce that $\tilde{d}_s = 1.91 \pm 0.11$ is close to the computed value above. From the expression of α (equation (15)), one can deduce that $\sigma \approx 1.5$. This value is in agreement with the notion that $\sigma > 1$ (Alexander *et al* 1993).

If we suppose that in the $q\lambda \gg 1$ limit the dynamic structure factor is controlled by the scaling law (17a), by comparison with the computed δ and β, we find that $\tilde{d}_s \approx 1.97$ and

$\sigma \approx 1$. The value of the obtained spectral dimension $\tilde{d}_s$ is close to the value deduced from the DOS spectra. This σ-exponent value differs from the $q\lambda \ll 1$ limit, but is still close to 1 as expected theoretically.

In conclusion, to take into account the tensorial nature of vibrations in realistic systems like silica aerogels, we have developed a model where the interaction between atoms is represented by the BKS potential. With a structure based on a DCLA fractal system, we have reproduced the density of states of spectra obtained for silica aerogels. Two different contributions are observed, as in experimental conditions, with spectral dimensions $\tilde{d}_b \approx 1$ and $\tilde{d}_s \approx 2$ close to the measured values. In agreement with reality, we note that our model shows that the sound velocity in our systems increases with increasing macroscopic density. This model accurately reproduced the results obtained by inelastic neutron scattering in silica aerogels. Our model qualitatively and quantitatively gives a good description of the dynamic properties of silica aerogels. To obtain a complete description, studies on light scattering in silica aerogels with this model are in progress.

Acknowledgments

References

Alexander S 1989 *Phys. Rev.* B **40** 7953
Alexander S, Courtens E and Vacher R 1993 *Physica* A **195** 286
Alexander S and Orbach R 1982 *J. Physique Lett.* **43** L625
Anglaret E, Hasmy A, Courtens E, Pelous J and Vacher R 1994 *Europhys. Lett.* **28** 591
Anglaret E, Pelous J and Hrubesh L H 1995 *J. Non-Cryst. Sol.* **186** 137
Benoit C, Royer E and Poussigue G 1992 *J. Phys.: Condens. Matter* **4** 3125
Botet R, Jullien R and Kolb M 1983 *J. Phys. A: Math. Gen.* **17** L75
Courtens E, Pelous J, Phalippou J, Vacher R and Woigner T 1987 *Phys. Rev. Lett.* **58** 128
Courtens E and Vacher R 1997 *Amorphous Insulators and Semiconductors (NATO ASI Series)* ed M F Thorpe and
        M Mitkova (Dordrecht: Kluwer) pp 255–88
Courtens E, Vacher R, Pelous J and Woigner T 1988 *Europhys. Lett.* **6** 245
Feng S 1985 *Phys. Rev.* B **32** 5793
Feuston B P and Garofalini S H 1988 *J. Chem. Phys.* **89** 5818
Garofalini S H 1982 *J. Chem. Phys.* **76** 3189
Guillot B and Guissani Y 1997 *Phys. Rev. Lett.* **78** 2401
Hasmy A, Anglaret E, Foret M, Pelous J and Jullien R 1994 *Phys. Rev.* B **50** 6006
Hasmy A, Foret M, Pelous J and Jullien R 1993 *Phys. Rev.* B **48** 9345
Jullien R and Botet R 1987 *Aggregation and Fractal Aggregates* (Singapore: World Scientific)
Jund P and Jullien R 1999 *Phil. Mag.* A **79** 1 223–36
Jund P, Rarivomanantsoa M and Jullien R 2000 *J. Phys.: Condens. Matter* **12** 8777
Nakayama T, Yakubo K and Orbach R 1994 *Rev. Mod. Phys.* **66** 381
Rahmani A, C Benoit, Jullien R and Poussigue G 1998 *Phil. Mag.* B **77** 421
Rahmani A, Benoit C, Jullien R, Poussigue G and Sakout A 1996 *J. Phys.: Condens. Matter* **8** 5555
Rahmani A, Benoit C and Poussigue G 1994 *J. Phys.: Condens. Matter* **6** 1483
——1995 *J. Phys.: Condens. Matter* **7** 8903
Reichenauer G, Fricke J and Buchenau U 1989 *Europhys. Lett.* **8** 415
Stoll E, Kolb M and Courtens E 1992 *Phys. Rev. Lett.* **68** 2472
Tsuneyuki, Tsukada, Aoki and Matsui 1988 *Phys. Rev. Lett.* **61** 869
Vacher R, Courtens E, Coddens C, Heidemann A, Tsujimi Y, Pelous J and Foret M 1990 *Phys. Rev.* B **65** 1008
Van Beest B W H, Kramer G J and van Santen R A 1990 *Phys. Rev. Lett.* **64** 1955
Viliani G, Dell'Anna R, Pilla O, Montagna M, Roucco G, Signorelli G and Mazzacurati V 1995 *Phys. Rev.* B **52** 3346